

***In vivo* quantification of ER- β expression by pharmacokinetic modeling: Studies
with ^{18}F -FHNP PET**

I.F. Antunes¹, A.T.M. Willemsen¹, J.W.A. Sijbesma¹, A.S. Boerema^{1,2}, A. van Waarde¹,
A.W.J.M. Glaudemans¹, R.A.J.O. Dierckx¹, E.G.E. de Vries³, G.A.P. Hospers³ and E.F.J. de Vries¹

¹ *University of Groningen, University Medical Center Groningen, Nuclear Medicine & Molecular
Imaging and* ² *Medical Oncology, Groningen, The Netherlands*

² *University of Groningen, Groningen Institute for Evolutionary Life Sciences, Groningen, The
Netherlands*

³ *University of Groningen, University Medical Center Groningen, Medical Oncology, Groningen,
The Netherlands*

* Author for correspondence:

Inês F. Antunes, PhD, University of Groningen, University Medical Center Groningen, Dept. of
Nuclear Medicine and Molecular Imaging Groningen, The Netherlands, PO Box 30.001, 9700 RB
Groningen, The Netherlands, Tel.: +31-50-3615779, FAX: +31-50-3611687, Email:
i.farinha.antunes@umcg.nl

Running title: ***In vivo* quantification of ER- β**

Word count: 4955

ABSTRACT

The estrogen receptor (ER) is a target for endocrine therapy in breast cancer patients. Individual quantification of ER α and ER β expression, rather than total ER levels, might enable better prediction of the response to treatment. We recently developed the tracer 2-¹⁸F-fluoro-6-(6-hydroxynaphthalen-2-yl)pyridin-3-ol (¹⁸F-FHNP) for assessment of ER β levels with positron emission tomography (PET). Here we investigated several pharmacokinetic analysis methods to quantify changes in ER β availability with ¹⁸F-FHNP-PET. **Methods:** Male nude rats were subcutaneously inoculated in the shoulder with ER α /ER β -expressing SKOV3 human ovarian cancer cells. Two weeks after tumor inoculation, a dynamic ¹⁸F-FHNP-PET scan with arterial blood sampling was acquired in rats treated with vehicle or various concentrations of estradiol (non-specific ER agonist) or genistein (ER β selective agonist). Different pharmacokinetic models were applied to quantify ER β availability in the tumor. **Results:** Irreversible uptake compartment models fitted the kinetics of ¹⁸F-FHNP uptake better than reversible models. The irreversible 3-tissue compartment model, which included both the parent and the metabolite input function, gave comparable results as the irreversible 2-tissue compartment model with only a parent input function, indicating that radioactive metabolites contributed little to the tumor uptake. Patlak graphical analysis gave comparable metabolic rates (K_i) as compartment modeling. The K_i values correlated well with ER β expression, but not with ER α , confirming that K_i is a suitable parameter to quantify ER β expression. Standardized uptake values at 60 minutes after tracer injection also correlated ($r^2=0.47$; $P=0.04$) with ER β expression. A reduction in ¹⁸F-FHNP tumor uptake and K_i values was observed in the presence of estradiol or genistein. **Conclusion:** ¹⁸F-FHNP-PET enables assessment of ER β availability in tumor-bearing rats. The most suitable parameter to quantify ER β expression is the K_i . However, a simplified static imaging protocol for determining the standardized uptake values (SUV) can be applied to assess ER β levels.

Keywords: Estrogen-receptors, pharmacokinetics, PET, quantification, oncology

INTRODUCTION

The estrogen receptors are involved in the development and progression of hormone-sensitive cancers. The ER operates as ligand-dependent transcription factor that modulates oncogenesis and inhibits tumor suppressor genes. The ER is a key target in endocrine therapies, aiming to inhibit hormone signaling in hormone-sensitive cancers (1). The ER consists of 2 isoforms: ER α and ER β , which have opposite physiological effects. Activation of ER α by estrogens induces cell proliferation and cell survival, while activation of ER β leads to the formation of a heterodimer ER α -ER β complex that inhibits ER α signaling and promotes apoptosis (2). Expression of ER β was suggested to be an independent predictive marker for benefit from tamoxifen treatment in patients with ER α -negative breast tumors, in which tamoxifen treatment is usually considered to be ineffective (3).

Currently, the primary surgical specimen or a tumor biopsy is used to assess ER tumor status. However, receptor expression in the tumor can change over time. Crosstalk of the ER with the growth factor receptors can also lead to changes in ER expression (4,5). Since ER α and ER β can induce opposite effects and ER status can convert overtime, either spontaneously or induced by treatment, a suitable tool to determine ER phenotypes of all lesions in a patient would be of great importance. Currently, 17 β -¹⁸F-fluoro-16 α -estradiol (FES) is used as a PET tracer for assessment of the ER status of breast cancer metastases. ER imaging can have an important impact on patient management, as FES-PET was shown to be responsible for a change in the intended treatment in a high percentage of patients presenting with a diagnostic dilemma (6). However, FES has poor subtype selectivity and therefore does not provide information about the ER subtype. Subtype-selective PET tracers would enable better characterization of tumor lesions and therefore, better assessment of their sensitivity towards endocrine therapies. ER β selective tracers might also be of interest for the assessment of the ER β in lung carcinomas and lung

fibrosis (7,8). Furthermore, imaging of ER subtypes may provide more insight in the mechanisms of resistance to hormonal treatment and crosstalk of ER with other signaling pathways.

Recently, we developed the PET tracer 2-¹⁸F-fluoro-6-(6-hydroxynaphthalen-2-yl)pyridin-3-ol (¹⁸F-FHNP), which selectively binds to ER β (9). However, ¹⁸F-FHNP uptake in the tumors was relatively low compared to ¹⁸F-FES uptake. Possible explanation for the observed low tumor uptake are low ER β expression in the tumor, low influx (K₁) due to poor perfusion or rapid metabolism of the tracer. To discriminate between these possible explanations, we further analyzed the metabolism of ¹⁸F-FHNP and its pharmacokinetics in tumor bearing rats. To assess the validity of ¹⁸F-FHNP-PET for imaging of ER β expression, several imaging parameters were correlated with the ER β expression levels, as determined by Western blotting.

MATERIALS AND METHODS

Synthesis of ¹⁸F-FHNP

¹⁸F-FHNP was prepared as previously described (9). ¹⁸F-FHNP was obtained within 115 minutes in 9 \pm 4 % radiochemical yield (decay corrected, based on ¹⁸F-fluoride). Quality control was performed by ultra-performance liquid chromatography, using a HSS-T3 column (1.8 μ m, 3.0x50 mm) with 30% aqueous acetonitrile as the mobile phase at a flow of 1 mL/min. At the end of synthesis the molar activity was 378 \pm 84 GBq/ μ mol and the radiochemical purity was always > 98%.

Animals

Male nude rats were obtained from Harlan (Lelystad, The Netherlands, n=32). The animals were provided with standard laboratory chow and tap water *ad libitum*. All studies were carried out in compliance with the Dutch law and local ethical guidelines for animal experiments. The protocol was approved by the Institutional Animal Care and Use Committee (DEC 6657B).

After at least 1 week of acclimatization, SKOV3 cancer cells [10^6 cells in a 1:1 mixture of Matrigel and Dulbecco's Modified Eagle Medium-high with 10% fetal bovine serum] were subcutaneously injected into the upper back of the rats. Approximately 15 days after inoculation, palpable tumor nodules were formed. The animals were randomly divided into different groups: Controls (n=9); animals administered with different concentrations of the non-specific ER agonist estradiol (n=14) or animals administered with the ER β specific agonist genistein (n=9).

Pet Imaging

Two weeks after tumor inoculation, a 60-minutes dynamic PET scan with arterial blood sampling was performed. The animals were anesthetized with isoflurane (5% for induction and 2% for maintenance) and a cannula was inserted in the femoral artery for blood sampling and a second cannula was inserted in the femoral vein for tracer injection. The animals were carefully positioned in the PET camera (MicroPET Focus 220, Siemens) with their tumors in the center of the field-of-view. A transmission scan of 515 seconds with a Co-57 point source was obtained for the correction of attenuation and scatter. A mixture of ^{18}F -FHNP (15.7 ± 4.6 MBq, 1 mL) with estradiol [0.3 $\mu\text{g/g}$ (n=4), 0.03 $\mu\text{g/g}$ (n=5), 0.003 $\mu\text{g/g}$ (n=5)] in phosphate buffer saline or vehicle (n=5) was injected via the femoral vein using an injection pump set at a flow rate of 1 mL/min. In another group of animals, genistein [5 $\mu\text{g/g}$ (n=5) and 0.5 $\mu\text{g/g}$ (n=4)] in 50% aqueous ethanol or vehicle (n=4) was intraperitoneally administered 5 minutes before tracer injection (9). The highest concentration of estradiol was chosen based on previous studies, in which effective blocking of ^{18}F -FES was achieved in rats (10). Due to solubility issues, the highest dose of genistein was 5 $\mu\text{g/g}$, similar to what was previously used in mice (9). Immediately after intravenous administration of ^{18}F -FHNP, a 60-min emission scan was started and blood samples of 0.1 mL were taken at approximately 10, 20, 30, 40, 50, 60, 90, 120, 150, 180, 300, 450, 600, 750, 900, 1200, 1500, 1800, 2400, 3000 and 3600 seconds after injection. After collection of each blood sample, 0.1 mL of heparinized saline was injected through the femoral artery to prevent

large changes in blood pressure. A 25 μL aliquot of blood was collected from each sample. The remaining blood was centrifuged (3461 g for 5 min) and a 25 μL aliquot of plasma was collected, whereas the remaining plasma was used for metabolite analysis. Radioactivity levels in the blood and plasma samples were measured with a well counter (LKB Wallac, Turku, Finland) and used to create the arterial input functions. Immediately after completion of the PET scan, the animals were terminated with an excess of isoflurane anesthesia and the bed containing the animal was positioned in a computed tomography (CT) scanner (MicroCT II, CTI, Siemens). A CT image was acquired for 15 min for anatomic localization of the tumor. After the CT scan, the tumors were excised and kept at $-20\text{ }^{\circ}\text{C}$ until further processing for Western blotting. CT imaging and Western blotting was performed as previously described (9).

Metabolite Analysis

50 μL of acetonitrile was added to approximately 25 μL of plasma sample to precipitate the plasma proteins. The samples were centrifuged at 16,000g for 3 min. A 2 μL aliquot of the supernatant was collected and applied on a thin-layer chromatography plate. The thin-layer chromatography plate was eluted with n-hexane/ethyl acetate (1:1) (R_f ^{18}F -FHNP = 0.7). After elution, radioactivity on thin-layer chromatography plates was analyzed by phosphor storage imaging. Exposed screens were scanned with a Cyclone phosphor storage system (PerkinElmer) and the percentage of intact ^{18}F -FHNP as a function of tracer distribution time was calculated by region-of-interest analysis using OptiQuant Software.

Image Reconstruction and Data Analysis

List mode data of the emission scans was separated into 21 frames (6×10 , 4×30 , 1×120 , 3×150 , 3×300 and 4×600 seconds). Emission sinograms were iteratively reconstructed (ordered subsets expectation maximum 2d, 4 iterations, 16 subsets) after being normalized and corrected for attenuation, scatter and radioactive decay. The CT and PET images were fused using Inveon

Research Workplace software (Siemens Preclinical Solutions, Knoxville, TN) and a volume of interest covering the whole tumor was manually drawn on the CT images and transferred to the corresponding PET images. The last 9 frames of the PET images were summed (10-60 minutes) and a second volume of interest of the viable part of the tumor was generated automatically with 20% of the maximum tumor uptake as the threshold using a region growing method. The resulting volumes of interest were used on the original dataset (0-60 minutes) to generate the corresponding time-activity curves, using standard software (Inveon, Siemens, Knoxville, TN). Tracer accumulation in tumors is expressed as standardized uptake value, which is defined as (assuming that all measured tissues have a density of 1g/mL):

$$SUV = \frac{\text{Tissue activity concentration (MBq/g)} \times \text{body weight (g)}}{\text{Injected dose (MBq)}}$$

Pharmacokinetic Modeling

Compartmental methods. Since plasma metabolite analysis showed that ¹⁸F-FHNP is rapidly transformed into polar metabolites, it seemed likely that they could contribute to activity in the tumors and thus might introduce a bias in the analysis. Thus, to calculate the pharmacokinetic parameters in this study, 2 model configurations were applied: i) a 3-tissue compartment model (3TCM) consisting of an irreversible 2-tissue model for the parent fraction and a reversible 1-tissue model for the metabolite fraction (2 input functions, Fig.1A) and ii) an irreversible 2-tissue compartment model (2TCM), neglecting the presence of radioactive tissue metabolites (1 input function, Fig.1B). Pharmacokinetic modeling of tracer kinetics in the tumor was performed using PMOD software (Version 3.3). The plasma, blood and metabolite activity curves were corrected for decay. In the 3TCM, both the metabolite-corrected plasma curve and the metabolite plasma curve were used as the input functions. In the 2TCM, the metabolite-corrected plasma curve was used as input function. In both models, the whole blood curve was used for blood volume

correction. Blood volume (V_B) in the tumor was a free modeling parameter. The whole blood, parent ^{18}F -FHNP and metabolite input functions were obtained from each individual animal.

Graphical methods. Graphical analysis methods are simplified linear approximations of compartment modeling approaches that often can provide more robust estimates of relevant uptake parameters. The dynamic PET data was subjected to Patlak graphical analysis (for irreversible tracer binding), using the metabolite-corrected plasma time-activity curve as input function (11). This graphical analysis yields slope values equivalent to K_i , the irreversible uptake rate constant.

Model selection. The model that could best fits tracer kinetics in the tumor was selected on the basis of the Akaike information criterion (AIC) for small sample sizes and model robustness (12).

Standardized uptake values. In order to assess whether ER β expression could also be estimated from static PET data, the SUV was calculated from the last frame (50-60 minutes) of the ^{18}F -FHNP scan.

Statistical Analysis

Statistical analyses were performed with Excel 2003 (Microsoft) and Graphpad Prism (version 5.04). Differences between pharmacokinetic models were analyzed using a two-sided paired Student's t-test. Differences in tracer accumulation between controls and different concentrations of blocker were analyzed using a two-sided unpaired Student's t-test. Significance was reached when the probability (P) value was ≤ 0.05 . Correlations were calculated with the linear regression algorithm in Graphpad Prism (version 5.04) and were considered statistically significant whenever $r^2 > 0.5$ and $P < 0.05$. Throughout the manuscript values are presented as mean \pm the standard error of the mean .

RESULTS

PET Images

All rats developed a large SKOV3 xenograft ($1.87 \pm 0.98 \text{ cm}^3$) without estradiol administration. Due to their large size, tumors became partially necrotic, with $24 \pm 19\%$ of the tumor volume being non-viable. Necrotic areas were clearly visible, as ^{18}F -FHNP scans showed low uptake in the non-viable parts of the tumor (Fig. 2A).

^{18}F -FHNP Kinetics in Tumor and Plasma

The kinetics of ^{18}F -FHNP uptake in SKOV3 xenografts are presented in Fig. 2B. Tracer uptake in the tumors reached a maximum within the first minute after tracer injection. This peak uptake was followed by a plateau within 10 minutes with no appreciable washout within the duration of the scan.

Metabolite analysis revealed that only 6% of the total plasma radioactivity consisted of intact ^{18}F -FHNP at 5 min post injection, which decreased to only 0.5% at 60 min (Fig. 3A). ^{18}F -FHNP kinetics in plasma (metabolite-corrected, Fig. 3B) indicated a rapid mono-exponential tracer clearance with a half-life of $0.29 \pm 0.06 \text{ min}$.

Pharmacokinetic Analysis

Both control groups used for the blocking experiments were combined for pharmacokinetic analysis. For the initial analysis of the tumor kinetics in control animals ($n=9$) by compartment modeling, the reversible and irreversible 2TCM were applied. Both models could be fitted to the data with no significant difference in the AIC values (data not shown). However, when the reversible model was used, most k_4 values were close to zero. Therefore, the irreversible model was then evaluated with either one (parent; 2TCM) or two (parent and metabolite; 3TCM) input functions. The AIC values were 84 ± 14 and 90 ± 16 for the 3TCM and 2TCM, respectively. However, neither model was significantly better than the other ($P= 0.14$). When comparing the individual parameters (K_1 , k_2 , k_3 and K_i) obtained from the 2TCM with the corresponding parameters obtained from 3TCM, no significant differences were found (Table1).

In addition, K_i obtained from both TCM were highly correlated ($r^2=0.89$, $P=0.0001$, Fig. 4) as well as the k_3 values ($r^2=0.864$, $P=0.0003$) and to a less extent the K_1 values ($r^2=0.644$, $P=0.0092$). However, the 3TCM tends to give less robust values, as more variables need to be assessed.

Patlak graphical analysis provided K_i values (Fig. 5) that correlated strongly with the K_i obtained from the 2 TCM ($r^2=0.93$, $P<0.0001$) and to a lesser extent with K_i values from the 3TCM ($r^2=0.71$, $P=0.004$). SUV showed reasonably good correlations with K_i values obtained from the 2TCM ($r^2=0.73$, $P=0.004$), 3TCM ($r^2=0.63$, $P=0.011$), and Patlak analysis ($r^2=0.60$, $P=0.014$) (Supplemental Fig. 1).

Correlation of Imaging with ER Expression

Western blotting was performed to quantify the ER β and ER α expression in the SKOV3 xenografts (controls, $n=9$). Immunoreactive bands for ER β and ER α were visualized at 55kDa and 66kDa, respectively. The ER α / β -actin ratio (0.17 ± 0.15) in the tumor was 3 times higher than the ER β / β -actin ratio (0.06 ± 0.05). As shown in Fig. 6, the K_i of ^{18}F -FHNP obtained from the 2TCM correlates well with the ER β / β -actin ratio ($r^2=0.80$, $P=0.001$), but has no correlation with the ER α / β -actin ratio.

A similar correlation was obtained when ER β / β -actin ratios were compared to the K_i values obtained from Patlak graphical analysis ($r^2=0.68$, $P=0.006$) and with the K_i values from kinetic analysis using the 3TCM ($r^2=0.72$, $P=0.004$). These findings demonstrate that the K_i of ^{18}F -FHNP is a reflection of the ER β levels in the tumor. In addition, a moderate correlation between the SUV and the ER β levels in the tumor ($r^2=0.47$, $P=0.04$) was found.

Pharmacokinetic Analysis in the Presence of ER Ligands

In the second phase of the study, the analysis of ^{18}F -FHNP tumor kinetics using the 2TCM was performed in animals which were administered with different concentrations of the ER ligands estradiol (non-specific) or genistein (ER β selective). As shown in Table 2, a dose-dependent reduction in K_i in the tumors was observed. The reduction was only statistically significant at the highest dose of estradiol or genistein. A similar competition effect could also be observed when tracer uptake was obtained from a static scan and quantified as SUV (Supplemental Fig. 2). There was a good correlation between the K_i values and the SUV values ($n=32$; $y= 18.46x + 0.073$, $r^2=0.69$, $P<0.0001$).

DISCUSSION

In this study we confirmed that ER β expression can be quantified with ^{18}F -FHNP PET. The imaging parameter that correlated best with ER β expression was the influx rate, K_i . However, SUV values also correlated moderately with ER β .

ER β was suggested to be an independent biomarker for benefit from tamoxifen treatment or chemotherapy in patients with ER α negative breast tumors (3,13). Thus, a proper measurement of ER β activity might enable prediction of response to treatment. Unfortunately, immunological assays (standard method to measure ER levels) of ER β by immunohistochemistry can only provide information about a small part of a single lesion. PET imaging, on the other hand, can offer information about the receptor expression in all lesions in the patient. Previously there have been several attempts to develop a PET tracer for ER β , such as: 5- ^{18}F -fluoro-(2R*,3S*)-2,3-bis(4-hydroxyphenyl)pentanenitrile (^{18}F -FEDPN), 8 β -(2- ^{18}F -fluoroethyl)estradiol (^{18}F -BFEE $_2$) and 7- ^{76}Br -bromo-2-(4-hydroxyphenyl)benzodioxazol-5-ol (^{76}Br -Br-041) (14,15). However, these tracers failed to provide evidence of ER β -mediated uptake. Recently we have shown that ^{18}F -FHNP possesses ER β selectivity (9). To our knowledge, the current study was the first study

where ER β levels were quantified with pharmacokinetic modeling *in vivo* by a non-invasive imaging modality.

Metabolite analysis of plasma showed rapid conversion of ^{18}F -FHNP into a polar metabolite. Its metabolism rate (6% intact tracer at 5 minutes) in rats was faster than that of ^{18}F -FES (50% intact tracer at 6 minutes) (10). Thus, the fast metabolism of ^{18}F -FHNP can contribute to its low uptake in the tumors. If ^{18}F -FHNP possesses affinity towards circulating sex-hormone binding globulin (SHBG), the tracer will be protected from degradation in patients and the metabolism rate will likely be slower than in rodents (that lack SHBG), as was observed for ^{18}F -FES (16). Moreover, ^{18}F -FHNP is rapidly taken up by the tumor (within 1 minute), whereas the washout of the tracer from the tumor is slow, suggesting irreversible binding. When attempting to fit ^{18}F -FHNP data to the reversible 2TCM, very low values of k_4 were obtained, confirming that ^{18}F -FHNP behaves like an irreversible PET tracer. Irreversible tracer binding was also found for other PET tracers for hormone receptor imaging, such as ^{18}F -fluorodihydrotestosterone (^{18}F -FDHT) (17).

In pharmacokinetic modeling of irreversible tracers, the calculated parameters K_1 , k_2 , k_3 and the K_i are usually obtained from 1 or 2-tissue compartment analysis, assuming no contribution of metabolites to target tissue activity. These models may be adequately applied in neuroimaging due to the inability of polar metabolites to pass the blood brain barrier. However, when analyzing tumors, metabolites may contribute to tumor activity. Since ^{18}F -FHNP had a high rate of metabolism, it was crucial to evaluate the contribution of metabolites to the uptake in the tumor. Therefore, we tested a 3TCM that takes the presence of metabolites into account. As depicted in figure 4, the contribution of the metabolites to the total activity in the tumor is low ($12\pm 5\%$). When comparing the 3TCM with the 2 TCM, a good correlation between both methods was found for both k_3 and K_i . This suggests that, despite the high amount of metabolites in circulation, the uptake and trapping in the tumor is mainly due to the intact tracer. This is in agreement with observations for other hormone receptor tracers that were rapidly converted into

polar metabolites (mainly sulphates and glucuronides). These metabolites are polar, resulting in limited access into intracellular space, and therefore they do not significantly bind to the intracellular ER (17,18).

Graphical analysis gave similar results as compartment modeling, as the K_i values obtained from the Patlak analysis correlated strongly with the K_i values obtained in the 2TCM. Irrespectively of whether compartment modeling or graphical analysis is applied for the analysis, however, arterial blood sampling and metabolite analysis are recommended to obtain the K_i values. This may hamper clinical applicability. To avoid blood sampling, an input function could be extracted non-invasively from the blood pools of the PET dynamic images or by scaling an arterial blood population input function using a venous blood sample. However, these alternative methods would require validation. Thus, in this study, to further simplify data acquisition and analysis procedures, tracer uptake, expressed as SUV, obtained from a static scan without blood sampling was evaluated as a potential parameter to describe ER β expression. The SUV correlated well with K_i values obtained from kinetic analysis using the 2TCM. Simplified methods such as SUV, do not take into account possible influences of metabolite formation and V_B . This could explain why K_i correlated better with ER β expression than the SUV. Nevertheless, it was also observed in this study that the SUV values correlated moderately with ER β expression in the tumors. It is important to emphasize that K_i and SUV values only correlated with ER β expression in the tumors and not with ER α expression, confirming the selectivity of ^{18}F -FHNP for ER β .

^{18}F -FHNP metabolism and kinetics in blood and plasma were not affected by the presence of different concentrations of the ER ligands estradiol and genistein, suggesting that metabolism and clearance pathways were not saturated by the competitors (data not shown). When ^{18}F -FHNP was given with different concentrations of estradiol or genistein, a dose-dependent reduction in tracer uptake in the viable part of the tumor was observed. The K_i and SUV values correlated well for the different concentrations of ER ligands, indicating that changes

in ^{18}F -FHNP kinetics could be observed with both metrics. This suggests the possibility of using a simplified imaging protocol to estimate receptor availability that does not involve blood sampling.

It should be noted that the uptake of ^{18}F -FHNP is only 30% inhibited by estradiol or genistein. This low inhibition percentage most likely is correlated to the relatively low amount of ER β expression in these tumors. Low receptor expression yields only a low absolute amount of specific tracer binding. In contrast nonspecific binding is independent of receptor expression, as a consequence, the percentage of specific binding relative to the amount of nonspecific binding will be low. Therefore, it would be advisable to perform further studies in a more suitable model with tumors that display higher ER β expression levels. Moreover, one cannot exclude that the amounts of agonists used in these experiments were too low to completely saturate all receptors. Thus, higher concentrations of genistein and estradiol should also be tested in future studies.

CONCLUSION

In this study, we were able to prove that ^{18}F -FHNP trapping in the tumor is correlated with ER β expression, but not with ER α , which confirms the subtype selectivity of this PET tracer. The most suitable parameter to describe ER β expression with ^{18}F -FHNP-PET is the influx rate constant, K_i , when a dynamic PET acquisition protocol with arterial blood sampling and metabolite analysis is applied. However, simplification of the acquisition and analysis protocol is possible, as the SUV could also be applied to assess ER β levels.

DISCLOSURE

This study was part of the MAMMOTH project, funded by the Center for Translational Molecular Medicine (CTMM) in the Netherlands. No other potential conflict of interest relevant to this article was reported.

REFERENCES

1. Minutolo F, Macchia M, Katzenellenbogen BS, Katzenellenbogen JA. Estrogen receptor β ligands: recent advances and biomedical applications. *Med Res Rev.* 2011;31:364-442.
2. Fox EM, Davis RJ, Shupnik MA. ER β in breast cancer—onlooker, passive player, or active protector? *Steroids.* 2008;73:1039-1051.
3. Yan Y, Li X, Blanchard A, et al. Expression of both estrogen receptor-beta 1 (ER- β) and its co-regulator steroid receptor RNA activator protein (SRAP) are predictive for benefit from tamoxifen therapy in patients with estrogen receptor-alpha (ER- α)-negative early breast cancer (EBC). *Ann Oncol.* 2013;24:1986-1993.
4. Marcom PK, Isaacs C, Harris L, et al. The combination of letrozole and trastuzumab as first or second-line biological therapy produces durable responses in a subset of HER2 positive and ER positive advanced breast cancers. *Breast Cancer Res Treat.* 2007;102:43-49.
5. Smith IE, Walsh G, Skene A, et al. A phase II placebo-controlled trial of neoadjuvant anastrozole alone or with gefitinib in early breast cancer. *J Clin Oncol.* 2007;25:3816-3822.
6. van Kruchten M, Glaudemans AWJM, de Vries EFJ, et al. PET imaging of estrogen receptors as a diagnostic tool for breast cancer patients presenting with a clinical dilemma. *J Nucl Med.* 2012;53:182-190.
7. Niikawa H, Suzuki T, Miki Y, et al. Intratumoral estrogens and estrogen receptors in human non-small cell lung carcinoma. *Clin Cancer Res.* 2008;14:4417-4426.
8. Ikeda K, Shiraishi K, Yoshida A, et al. Synchronous multiple lung adenocarcinomas: estrogen concentration in peripheral lung. Yang F, ed. *PLoS One.* 2016;11:e0160910.
9. Antunes IF, Waarde A van, Dierckx RA, de Vries EGE, Hospers GAP, de Vries EF. Synthesis and evaluation of the new estrogen receptor β selective radioligand [^{18}F]FHNP:

- Comparison with [¹⁸F]FES. *J Nucl Med.* 2017;58:554-559.
10. Khayum MA, de Vries EFJ, Glaudemans AWJM, Dierckx RAJO, Doorduyn J. In vivo imaging of brain estrogen receptors in rats: A 16-¹⁸F-fluoro-17-estradiol PET study. *J Nucl Med.* 2014;55:481-487.
 11. Patlak CS, Blasberg RG, Fenstermacher JD. Graphical evaluation of blood-to-brain transfer constants from multiple-time uptake data. *J Cereb Blood Flow Metab.* 1983;3:1-7.
 12. Glatting G, Kletting P, Reske SN, Hohl K, Ring C. Choosing the optimal fit function: Comparison of the Akaike information criterion and the F-test. *Med Phys.* 2007;34:4285-4292.
 13. Elebro K, Borgquist S, Rosendahl AH, et al. High estrogen receptor β expression is prognostic among adjuvant chemotherapy-treated patients—results from a population-based breast cancer cohort. *Clin Cancer Res.* 2017;23:766-777.
 14. Yoo J, Dence CS, Sharp TL, Katzenellenbogen JA, Welch MJ. Synthesis of an estrogen receptor β -selective radioligand: 5-[¹⁸F]fluoro-(2R*,3S*)-2,3-bis(4-hydroxyphenyl)pentanenitrile and comparison of in vivo distribution with 16 α -[¹⁸F]fluoro-17 β -estradiol. *J Med Chem.* 2005;48:6366-6378.
 15. Lee JH, Peters O, Lehmann L, et al. Synthesis and biological evaluation of two agents for imaging estrogen receptor β by positron emission tomography: challenges in PET imaging of a low abundance target. *Nucl Med Biol.* 2012;39:1105-1116.
 16. Tewson TJ, Mankoff DA, Peterson LM, Woo I, Petra P. Interactions of 16 α -[¹⁸F]-fluoroestradiol (FES) with sex steroid binding protein (SBP). *Nucl Med Biol.* 1999;26:905-913.
 17. Beattie BJ, Smith-Jones PM, Jhanwar YS, et al. Pharmacokinetic assessment of the uptake of 16-¹⁸F-fluoro-5-dihydrotestosterone (FDHT) in prostate tumors as measured by PET. *J Nucl Med.* 2010;51:183-192.
 18. Mankoff DA, Tewson TJ, Eary JF. Analysis of blood clearance and labeled metabolites

for the estrogen receptor tracer [F-18]-16 alpha-fluoroestradiol (FES). *Nucl Med Biol.*
1997;24:341-348.

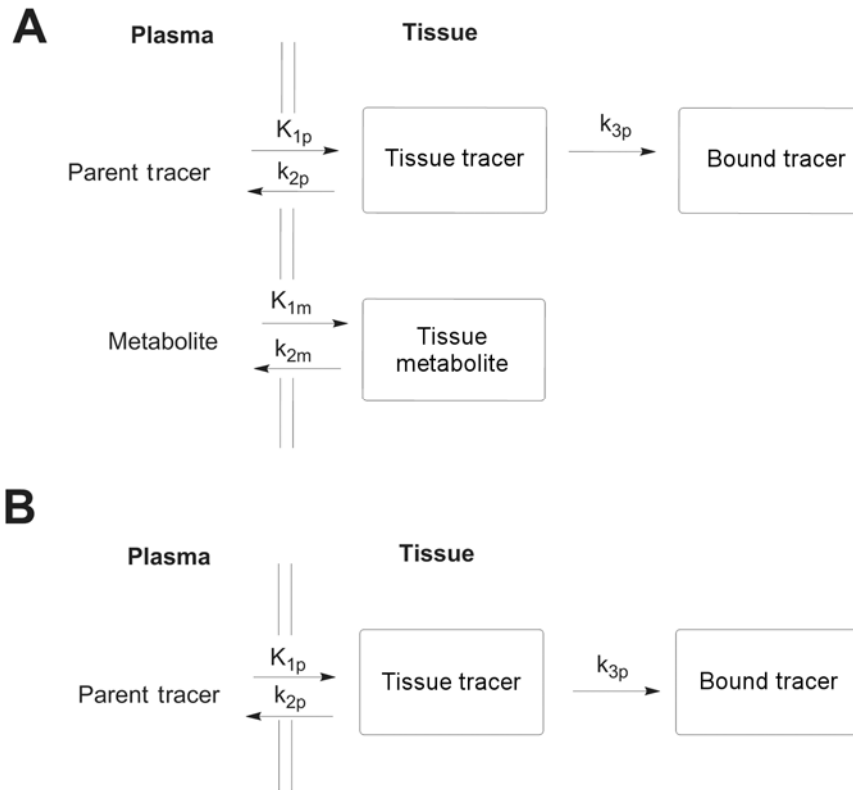


Figure1. Compartment models applied for ^{18}F -FHNP kinetic analysis. A) irreversible 3 tissue compartment model (3TCM) and B) irreversible 2-tissue compartment model (2TCM). Whereas K_{1p} = uptake constant of intact parent (mL/g/min); k_{2p} =clearance rate of intact parent (1/min); k_{3p} =selective binding of intact parent (1/min); K_{1m} =uptake constant of metabolites (mL/g/min) and k_{2m} =clearance rate of metabolites (1/min).

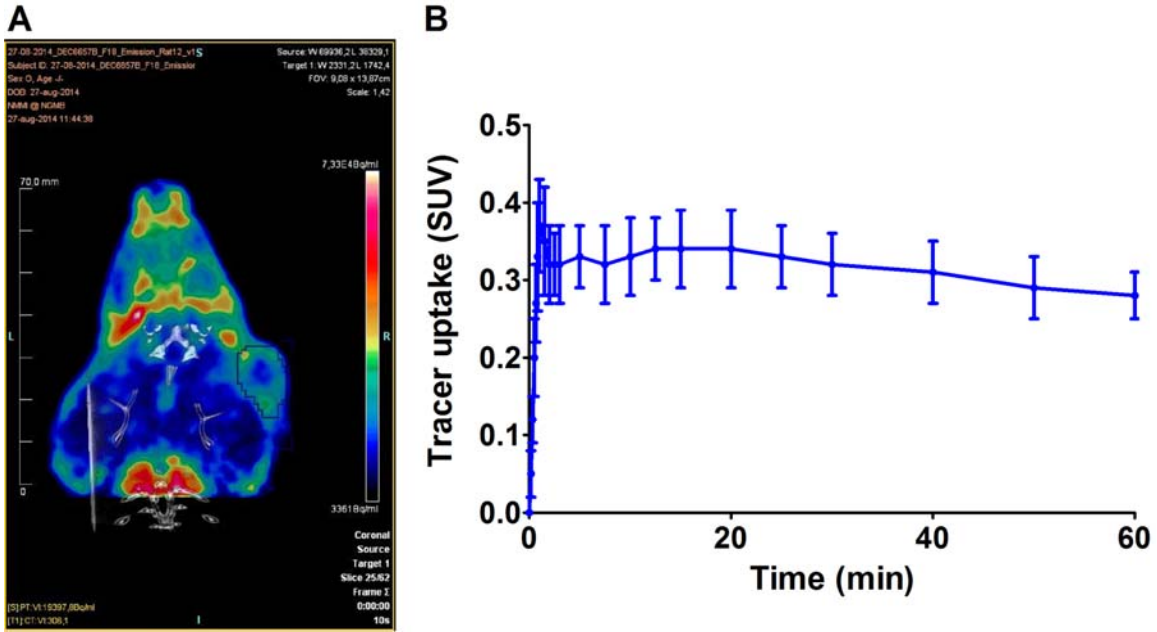


Figure 2. A) Coronal microPET/CT fusion images of a rat bearing a SKOV3 xenograft injected with ¹⁸F-FHNP (21.5 MBq). B) Averaged Time activity curve of ¹⁸F-FHNP uptake in SKOV3 xenografts (n=9).

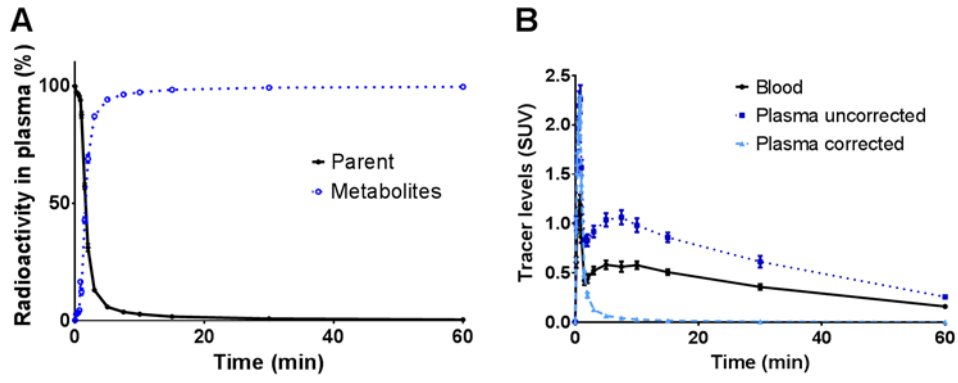


Figure 3. Metabolism (A) and metabolite-corrected plasma curves (B) for ^{18}F -FHNP.

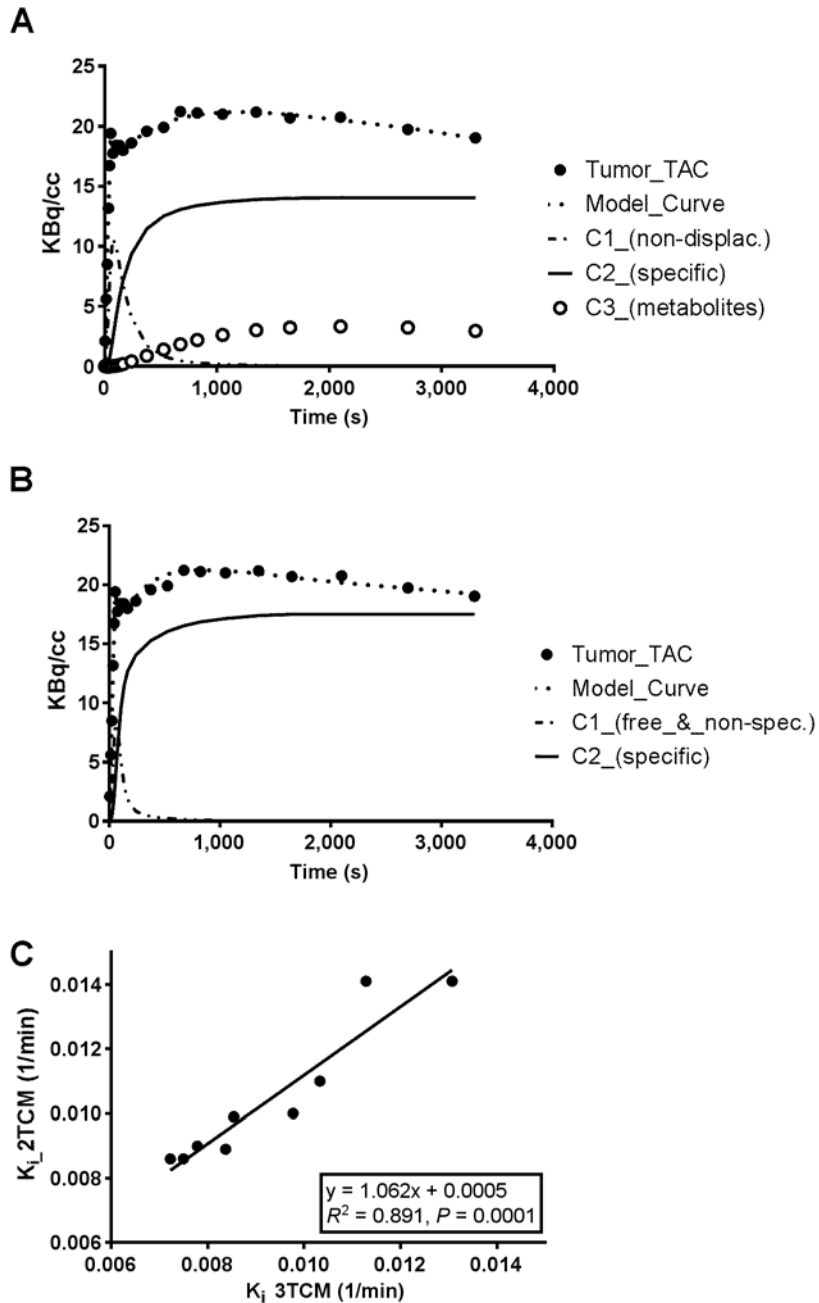


Figure 4. Representative examples of a ^{18}F -FHNP time-activity curve in a SKOV3 xenograft and the corresponding 3TCM (A) and 2TCM (B) fit, whereas C1, C2 and C3 stands for compartment 1, compartment 2 and compartment 3, respectively. C) Correlation between Influx constant (K_i) values from kinetic analysis using the 2TCM and 3TCM.

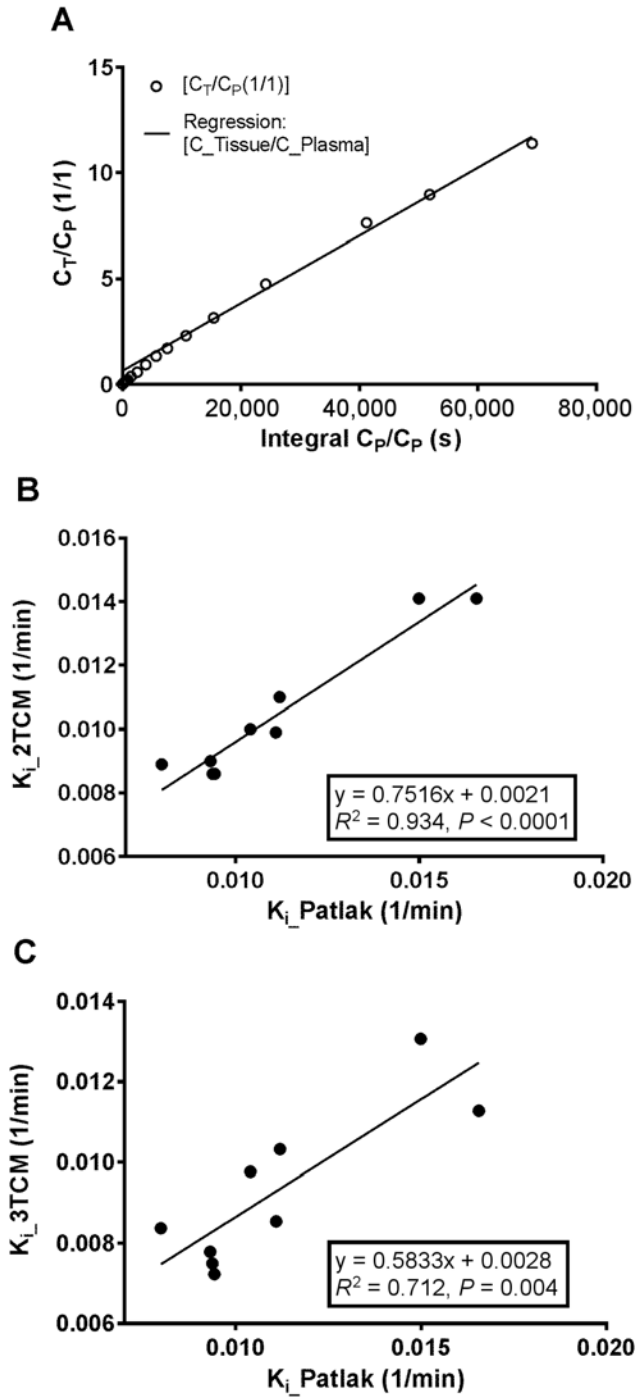


Figure 5. A) Representative image of Patlak graphical analysis of ^{18}F -FHNP uptake in a SKOV3 xenograft, whereas C_T and C_P stands for tissue and plasma compartment, respectively. Correlation between Patlak graphical analysis and K_i (Influx rate) values from kinetic analysis using B) the 3TCM or C) the 2TCM .

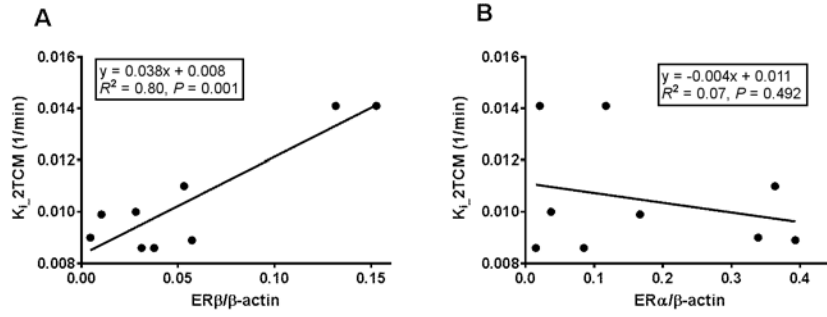


Figure 6. Correlation of the K_i values obtained from kinetic analysis using the 2 TCM (n=9) with ER β (A) and ER α (B) density obtained from the Western blotting assay

Table1. Summary of the k values of ^{18}F -FHNP obtained with the 2TCM and the 3 TCM (control group, n=9) and its AIC values.

Model	2TCM	3TCM	
	(parent)	(parent)	(metabolite)
V_B	0.017±0.008	0.016±0.069	
K_1 (mL/g/min)	0.022±0.010	0.0315±0.020	0.023±0.043
k_2 (1/min)	1.069±2.619	1.391±2.527	1.706±2.711
k_3 (1/min)	0.584±1.105	0.431±0.493	-
K_i (1/min)	0.010±0.002	0.0093±0.002	-
AIC	90.3±15.8	85±14.6	-

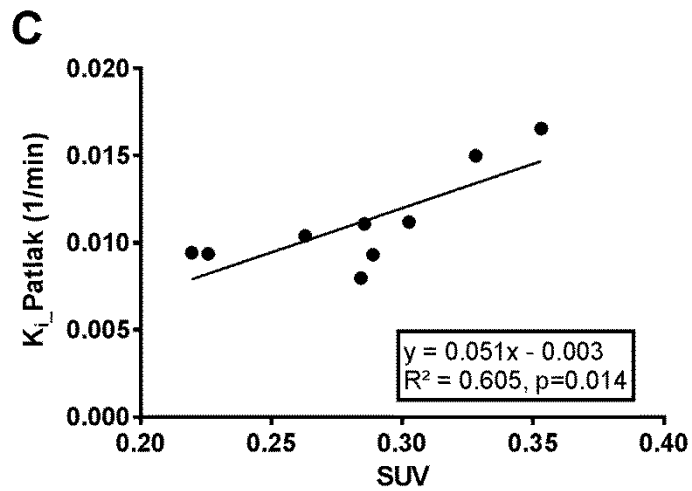
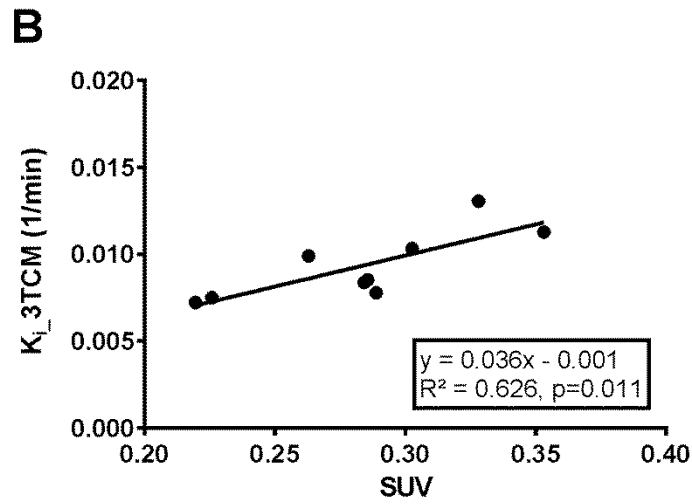
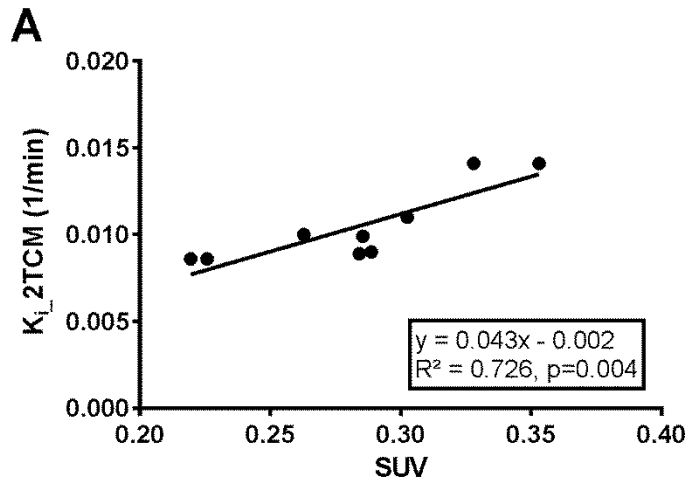
Table2. Comparison of the SUV values obtain from the PET data 50-60 minutes after injection of ¹⁸F-FHNP and the K_i (1/min) values obtained from the 2TCM fit for all groups.

	SUV	K _i _2TCM (1/min)
estradiol		
Control (n=9)	0.28±0.04	0.0105±0.0020
0.003µg/g (n=4)	0.26±0.05	0.0105±0.0034
0.03µg/g (n=5)	0.25±0.06	0.0100±0.0030
0.3µg/g (n=5)	0.18±0.05*	0.0073±0.0020*
genistein		
Control (n=9)	0.28±0.04	0.0105±0.0020
0.5µg/g (n=5)	0.25±0.01	0.0082±0.0014
5µg/g (n=4)	0.21±0.03*	0.0076±0.0011*

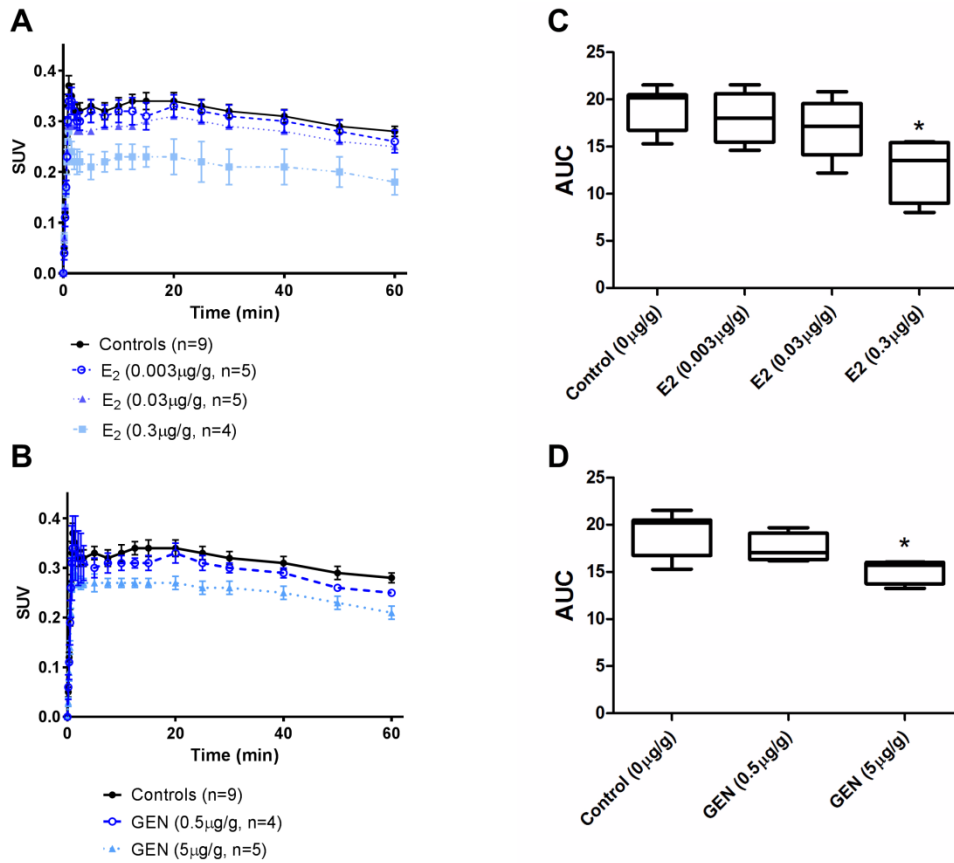
**P*<0.05 when compared to controls.

SUPPLEMENTAL MATERIAL

SUPPLEMENTAL FIGURES



Supplemental figure 1. Correlation between SUV and K_i values from kinetic analysis using A) the 2TCM; B) the 3TCM or C) Patlak graphical analysis performed on the same tumors.



Supplemental figure 2. Kinetics of ¹⁸F-FHNP in the SKOV3 xenografts. The effect of A) estradiol (E₂) and B) genistein (GEN) doses on tracer kinetics in the tumor over time. The effect of: C) estradiol and D) genistein on the area under the curve (AUC, min) for the different experimental groups. * p<0.05 when compared to the control group.